Structural Engineering and Mechanics, *Vol. 72, No. 6 (2019) 723-736*
DOI: https://doi.org/10.12989/sem.2019.72.6.723

Rehabilitation and strengthening of exterior RC beam-column connections using epoxy resin injection and FRP sheet wrapping: Experimental study

Comingstarful Marthong*

Department of Civil Engineering, National Institute of Technology Meghalaya, Shillong 793003, India

(Received October 20, 2018, Revised May 14, 2019, Accepted August 5, 2019)

Abstract. The efficacy of a technique for the rehabilitation and strengthening of RC beam-column connections damaged due to cyclic loading was investigated. The repair mainly uses epoxy resin infused under pressure into the damaged region to retrieved back the lost capacity and then strengthening using fiber reinforced polymer (FRP) sheets for capacity enhancement. Three common types of reduced scale RC exterior beam-column connections namely (a) beam-column connection with beam weak in flexure (BWF) (b) beam-column connections with beam weak in shear (BWS) and (c) beam-column connections with column weak in shear (CWS) subjected to reversed cyclic loading were considered for the experimental investigation. The rehabilitated and strengthened specimens were also subjected to similar cyclic displacement. Important parameters related to seismic capacity such as strength, stiffness degradation, energy dissipation, and ductility were evaluated. The rehabilitated connections exhibited equal or better performance and hence the adopted rehabilitation strategies could be considered as satisfactory. Confinement of damaged region using FRP sheet significantly enhanced the seismic capacity of the connections.

Keywords: Beam-column connections; Rehabilitation; Strengthening; Epoxy resin; FRP; Seismic capacity; Damage assessment

1. Introduction

Beam-column connection is one of the vital structural parts, whose behaviour during earthquake is very critical. The beam-column connection comprises of the joint plus the columns, beams, and slab adjacent to the joint (ACI 352R-02, 2002) and many times the connections become weak due to (a) inadequate anchorage of beam's reinforcement, (b) flexural reinforcement may be insufficient at the beam, (c) poor confinement of reinforcement and chances of failure during seismic attack. The behaviour of reinforced concrete (RC) moment resisting frame structures in the past earthquakes all over the world has highlighted the consequences of poor performance of beam column connections (Uma and Jain, 2006). Exterior connection which is confined by only two or three framing beams had suffered more in comparison to the interior ones. The failure of these connections during past earthquakes opened a new research direction in the field of rehabilitation and strengthening of beam-column connection for retrieving the lost capacity and enhanced future seismic safety. After an earthquake, a building may suffer damages and depending on the extent of damage repair and strengthening can be carried out on the damage area only. However, severely damaged structures are thought to be irreparable and are abandoned in spite of huge economic loss. To ensure further usability of the damaged structure, effective and reasonable rehabilitation techniques are needed to be investigated.

*Corresponding author, Ph.D., Associate Professor
E-mail: commarthong@nitm.ac.in

Several techniques for rehabilitation and strengthening of damaged connections were reported (Engindeniz *et al.* 2005). Of the various techniques, the most commonly used were jacketing with concrete and steel. However, these techniques possess its own practical limitations like labour intensive, artful detailing, increased dimension of structural element, susceptibility to corrosion etc. To overcome the mentioned difficulties, fiber-reinforced polymers (FRP) are widely used confinement materials for civil infrastructure applications because many theoretical and experimental studies have proved that FRP composite jackets can significantly increase strength and ductility of concrete structures. Apart from increasing the strength and ductility, FPR are most attractive for their tailorability. ACI Committee 440.2R (2002) were the basic guidelines followed by many researchers for the design of externally bonded FRP Systems for Strengthening Concrete Structures. The use of epoxy-bonded FRP sheets or strips as confining materials for repair or strengthening of RC beam-column connection has been reported by various researchers (Mosallam 2000, Ghobarah and said 2002, Karayannis and Sirkelis 2002, Mukherjee and Joshi 2005, Tsonos 2008, Karayannis and Sirkelis 2008, Karayannis *et al*. 2008, Saleh *et al*. 2010, Sasmal *et al.* 2010, Alsayed *et al.* 2010, Kakaletsis *et al*. (2011), Panda *et al.* 2013, Eslami and Ronagh, 2014, Tsonos 2014, Barbhuiya and Choudhury 2015, Hadi and Tran 2016, Ascione *et al.* 2017). They showed that seismic capacity and failure modes of the RC beam-column connections significantly improved. However, the effectiveness of any rehabilitation/strengthening techniques depends on the treatment provided to the fragmented concrete in the damaged region (Corazao and

http://www.techno-press.com/journals/sem&subpage=7
ISSN: 1225-4568 (Print), 1598-6217 (Online)

Durrani 1989, FEMA 308 1998, Karayannis 1998, Karayannis *et al*. 2008, Marthong *et al.* 2013). Hence, in this study an effort shall be focus on rehabilitating the affected damage zone of RC beam-column connections and strengthening using FRP sheet to improve their performance.

Several experimental studies have been carried out to evaluate the behavior of rehabilitated and strengthened RC beam-column connections subjected to cyclic loading. However, the comparative studies covering various common deficiencies namely, (a) beam-column connections with beam weak in flexure (BWF), (b) beam-column connections with beam weak in shear (BWS) and (c) beam-column connections with column weak in shear (CWS) were limited (Marthong *et al*. 2013, Bharbhuya and Choudhury 2015, Marthong *et al*. 2016). Thus, a holistic approach is to cover different deficient cases of RC beam-column connections so as to gather a comprehensive knowledge about the behaviour of these connections.

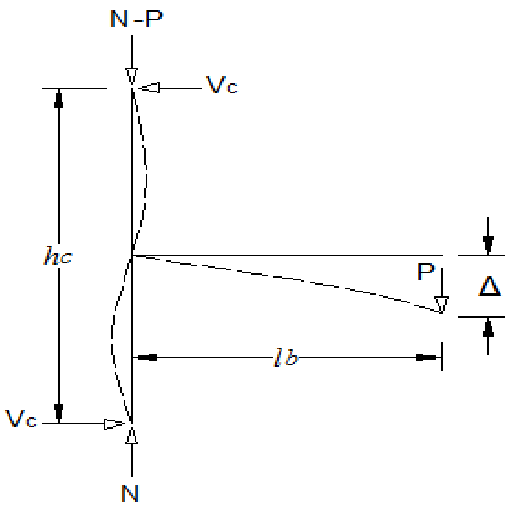

Fig. 1 Isolated exterior beam-column connection

2. Experimental program

2.1 Concrete specimens

A set consisting of three concrete cube (150x150x150), cylinder (150mm diameter and 300 mm height) and prism of 500x125x125 mm was used to evaluate mechanical strength of concrete specimens. Ordinary Portland Cement (OPC) of 53 grades conforming to IS: 12269 (1987) was considered. The maximum size of coarse aggregate was 12.5 mm. River sand was used as fine aggregate. Aggregates used have been tested as per relevant codes (IS: 2386a & b, 1963). Concrete mixes are designed for a characteristic cube compressive strength of 25 N/mm^2 which resulted in a target mean cube compressive strength of 31.6 N/mm^2 as per Bureau of Indian Standard (IS: 10262-2009) code provisions. All concrete mixes were produced with 383 kg/m^3 of cement, 720 kg/m^3 of fine aggregate, 1100 kg/m^3 of coarse aggregate, for a water-cement ratio of 0.5 and a compaction factor of 0.9.

2.2 Selection of RC beam-column connections

A free body diagram of an isolated exterior beam-column connection in its deformed position is shown in Fig. 1. It comprises of half height of a column at top and bottom as well as half of a beam length, which corresponded to the points of contra-flexure in beam and column under lateral loads. In this figure, h_c is the story height, l_b is half beam span corresponding to the length of the beam connected to the selected joint, N is the internal axial force of the column, P is the beam-tip load, V_c is the column shear force and Δ is the vertical beam-tip displacement. It may be noted that the symmetric boundary condition were maintained at both the ends of column for isolation of a single unit of beam-column connection. In this study, a typical full scale residential building with floor to floor height of 3.3 meters and the beam effective span of 3.0 meters were considered. For BWF and BWS specimens the dimension of beam and column was chosen as 300 mm x 360 mm and 300 mm x 300 mm respectively. Cross section analysis was based on the equilibrium equation and the moment carrying capacity of beam and column was calculated as 94.57 kN-m and 112.62 kN-m. The ratios of column-to-beam flexural capacity satisfy the criteria of strong column-weak beam condition (IS 13920-2016, ACI 318). While, to create a weak column the dimension of beam and column was chosen as 240 mm x 450 mm and 300 mm x 300 mm respectively and the moment carrying capacity of beam and column was calculated as 180.94 kN-m and 90.10 kN-m. The sub-assamblage is weak column-strong beam condition as per (IS 13920-2016, ACI 318). A 20 mm diameter high yield strength deformed (HYSD) bar was used for both beam and column as main reinforcement in all specimens. The beam-column connection was scaled down to one-third size for experimental investigation. Reinforcement and coarse aggregates were also geometrically scaled down for satisfying the similitude requirement.

2.3 Description of RC beam-column connections

The present study considered three typical deficiency namely, (a) beam-column connections with beam weak in flexure (BWF), (b) beam-column connections with beam weak in shear (BWS) and (c) beam-column connections with column weak in shear (CWS). Fig. 2 presented the reinforcement detailing of all the specimens. The longitudinal reinforcement consisted of high yield strength deformed (HYSD) bar of 8 mm diameter (Fe 500). A mild steel (MS) bar of 6 mm diameter (Fe 250) was also used as longitudinal as well as transverse reinforcement. The yield stress (MPa) and ultimate stress (MPa) for HYSD bars tested as per code provisions (IS 432 I 1982, IS 1608 1995) were found out to be 530 MPa and 620 MPa, while the same for Fe 250 bars were 285 MPa and 450 MPa respectively.

The detailing of BWF specimen is shown in Fig. 2a. Following the standard code of practice (IS 13920 2016, IS 456 2000) the beam specimen was designed as under reinforced section. A cross section of 100 mm x 100 mm and 100 mm x 120 mm for column and beam elements respectively was considered. HYSD bars of 8 mm diameter

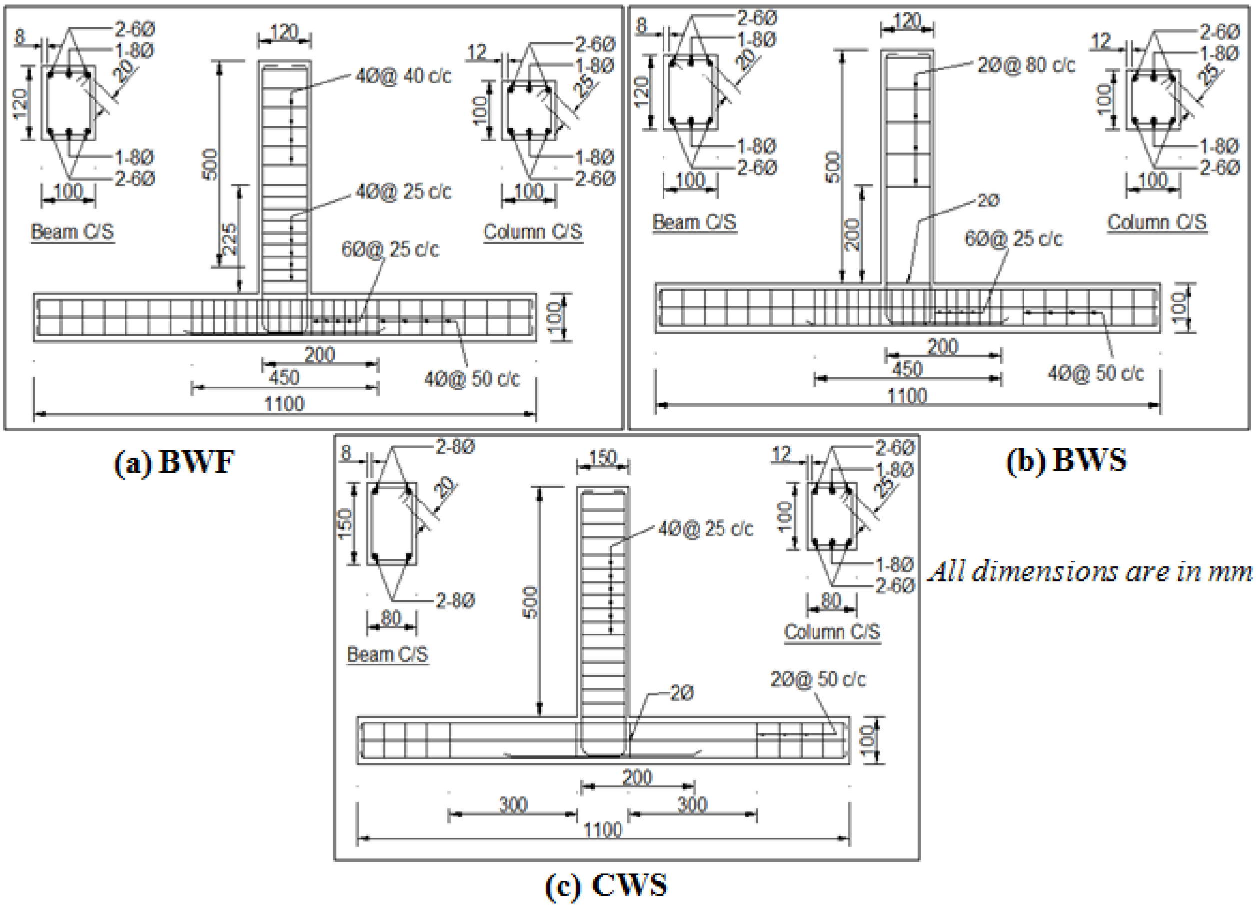

Fig. 2. Reinforcement detailing of specimens

and MS bar of 6 mm diameter were used as main bars in both column and beam. Following the code provision IS 13920 (2016) a lateral tie of 6 mm diameter MS bar at 25 mm c/c spacing was used in the special confinement zone of the column, while the remaining part was increased to 50 mm c/c. The shear reinforcement used in beam was of 6 mm diameter MS bar having spacing of 25 mm c/c near the beam-column joint for a length of 225 mm and a spacing of 40 mm c/c was provided in the remaining part.

The detailing of BWS specimens is shown in Fig. 2b. Under this category, the specimen was exactly similar in all respect to that of BWF specimen, except the shear reinforcement provided in beams. The amounts of shear reinforcements were reduced to make the beam weak in shear. To reduce the shear reinforcements in beam, lateral ties with 6 mm diameter bars with a spacing of 80 mm c/c were provided as shear reinforcement. To maintain the pre-defined failure location in the beam only the first two stirrups with a wider spacing of 200 mm c/c near the joint was placed.

Strong beam-weak column principle was followed for design of CWS specimen. The cross section of column as shown in Fig. 2c was kept same as that of BWF and BWS specimens, while the cross section of a beam was increased to 80 mm x150 mm. The main reinforcements in column were maintained similar to those of earlier cases, while same was increased in beam. In order to ensure the shear weakness of these specimens a wider lateral ties spacing of 300 mm c/c on either side of the joint region was provided. In the remaining part the spacing of lateral ties was reduced to 50 mm c/c. It may be mentioned that in all specimens a rectangular pattern lateral ties was adopted for a better response in terms of the developing failure mechanisms (Karayannis 2015). The detailed descriptions of all specimens are given in Table 1.

2.4 Casting of RC beam-column connections

Three sets of RC beam-column connections were cast. Each set consisted of two types of specimens namely BWF, BWS and CWS all these specimens were treated as control specimens. All specimens were cast with a concrete mix which has a mean cube compressive strength of not less than 31.6 MPa.

2.5 Materials / equipment for rehabilitation and strengthening of specimens

The materials used for repairing the damaged control specimens are low viscous epoxy resin (Conbextra EP10), micro concrete (Renderoc RG), concrete bonding agent (Nitobond EP) and Sealant material (Nitocote VF). All these materials were procured from Fosroc Chemicals (India) Pvt. Ltd.. Further, an injection pumps (hand operated) suitable for the injection of low viscous resins up to an injection pressure of 100 bar. Mechanical packers

Table 1 Descriptions of beam-column connections

Specimen	Beam			Column			$M_R = \frac{\sum M_C}{\sum M_B}$
	Span (mm)	Section (mm)	Longitudinal Reinforcement	Length (mm)	Section (mm)	Longitudinal Reinforcement	
BWF & BWS[a]	500	100×120	1-8 ϕ +2-6 ϕ -top 1-8 ϕ +2-6 ϕ -bottom	1100	100×100	2-8 ϕ +4-6 ϕ	2.38
CWS	500	80×150	2-8 ϕ -top 2-8 ϕ -bottom	1100	100×100	2-8 ϕ +4-6 ϕ	0.99

[a]*Beam weak in shear specimens have same dimensions and longitudinal reinforcement as that of beam weak in flexure specimens except the shear reinforcement provided in beam.*

M_R: ratio of column-to-beam flexural capacity

$\sum M_C$: sum of flexural capacities of the columns meeting at the joint under consideration
$\sum M_B$: sum of flexural capacities of beams at the same joint

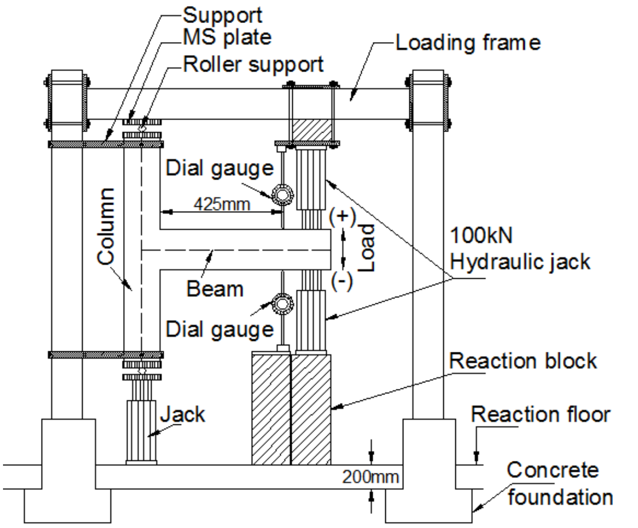

(a)

(b)

Fig. 3 Testing of beam-column connection (a) Test set-up (b) Actual testing arrangement

(type S, length of 70 mm and dia. of 13 mm) are used in the repairing works. The packers are drill-hole packers which are screwed into the drill-holes. When tightening the packers a fabric-reinforced rubber sleeve and firmly pressed against the drill-hole sides so that the packers can withstand even highest injection pressures in the drill-hole.

Woven sheets of glass friber reinforced plymer (GFRP) and carbon fiber reinforced polymer (CFRP) was used as a wrapping materials. The ultimate tensile strength for CFRP was found to be 630 N/mm^2 while the same for GFRP was found 315 N/mm^2. Modulus of Elasticity of CFRP and GFRP were found as 4.63×10^4 N/mm^2 and 1.167×10^4 N/mm^2 respectively. The mentioned properties are taken from the data sheet provided by the manufacturer. Nitowrap 30 (base and hardener) was used as primer coat and Nitowrap 410 (base and hardener) was used as saturant i.e. resin.

2.6 Test set-up and instrumentation

The setting of the test set-up and the actual testing arrangement is shown in Fig. 3. A loading frame of 500 kN capacity and hydraulic jack of 100 kN were used for applying the load to the specimens. In the test set-up, the column was positioned vertically while the beam is placed horizontally. In order to represent the gravity load, an axial load using hydraulic jack was applied to the column. The moments were approximately zero at the mid-span of the column when subjected to lateral loading. Roller supports were provided at both ends of the column in order to simulate the actual conditions of zero moments. The reversed loading was applied manually at a distance of 100mm from the free end of the beam by mean of two hydraulic jack mounted at the top and at the bottom. The hydraulic jack of 100 kN capacity was equipped with an in-built manually operated pumping units fitted with bourdon tube type load gauge and high-pressure flexible hose pipe. Two 100 mm range dial gauges were also placed at the top and bottom face of the beam tip to measure the vertical displacement of the beam.

2.7 Loading sequence

The present study considered the loading sequence followed by Vidjeapriya and Jaya (2013). In the loading sequences a displacement controlled mode was applied to the specimens. However, a one loading cycle at every amplitude of displacement was considered instead of three.

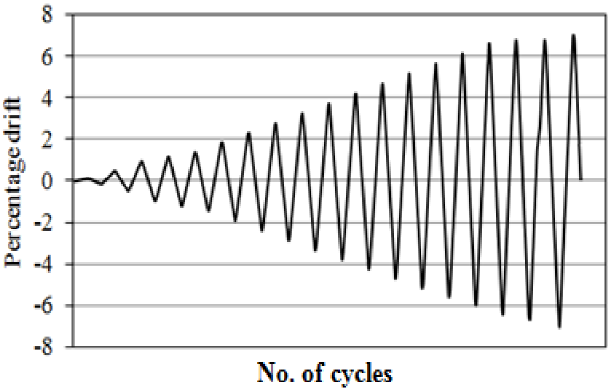

Fig. 4 Loading history

A maximum displacement of ±30 mm was applied in all the specimens. A typical loading history is presented in Fig. 4.

In order to utilize results obtained from cyclic loading test on structural elements for a general performance evaluation, there is a need to establish loading history that captures the critical issues of the element capacity as well as the seismic demand. The importance of loading sequence effects has not yet been established through research, and the sequence of large vs. small excursions in an element of a structure subjected to a severe earthquake does not follow any consistent pattern (Karayannis and Sirkelis, 2008). In the adopted loading, emphasis was given on the large inelastic excursion since they caused large damage and could lead quickly to ultimate state.

The ratio of beam tip displacement to the length of the beam measured from the joint to the position of the dial gauge is called the drift angle. Drift obtained by horizontally displacing the beam ends are equivalent to the inter-storey drift angle of a frame structure subjected to lateral loads. Two hydraulic jacks were mounted on top and bottom of the beam tip end to apply the reversed cyclic loading. As suggested by Ghobarah *et al*. (1997), an axial load of 10% of the gross capacity of the column was applied to the column end by utilizing a hydraulic jack to represent the dead load transferred from upper floors.

2.8 Rehabilitation and strengthening strategies

The repairing strategy was aimed to retrieve back the lost capacity of the damaged connections to their respective original seismic capacity. Thus, one damaged control specimens in each set of BWF, BWS and CSW were rehabilitated and designated as BWFRe, BWSRe and CWSRe respectively. Depending on the degree of damages, partial or complete replacement of loose concrete on the damaged area is necessary and followed by epoxy resin injection. Prior to epoxy injection, the voids created after removal of loose materials were patched or filled with micro concrete after a suitable bonding agent was applied on the clean surface for attaining adequate bond between old and freshly added concrete. Holes were drilled along cracks and packers were inserted through these holes, which served as filler neck for epoxy injection. Visible cracks were sealed and a low viscous epoxy resin was injected under high pressure into the cracked zone. Once the injected epoxy resin attained sufficient strength, the installed packers were removed and a grinding machine was subsequently used to remove the sealing materials. The typical repairing process is shown in Fig. 5.

Depending on the deficiency types, another set of damaged control specimens of BWF, BWS and CWS were rehabilitated as mentioned above and then wrap using FRP sheets as per the design configuration adopted by Chowdhury *et al*. (2013) which is shown in Fig 6a. These specimens were name as BWFR, BWSR and CWSR respectively. Strengthening of BWF specimens was carried out primarily to enhance the flexural capacity of the beam using CFRP. However, the increase in load carrying capacity led to the increase in shear force at any section of the beam. Thus, in order to ensure eventual flexural failure of the beam, shear enhancement of the beam was also done using GFRP. The joint was adequately strengthened with GFRP. BWS specimen eventually would fail in flexure which is the most preferred mode of failure. In order to strengthen the shear deficient the strengthening in the beam was done using GFRP as per the design configuration. A strip of one layer having width of 40 mm was wrapped around the beam with a spacing of 70 mm c/c. This strengthening scheme enhanced the shear capacity of the beam making it higher than the flexural capacity. Hence at this level the beam was expected to fail at the original flexural capacity of the control specimen, resulting a slight increment in the overall capacity. Further, flexural strengthening was also carried out to achieve an appreciable increase in capacity of the specimen. The flexural strengthening was carried with CFRP to such an extent that even after the flexural strengthening the beam fails in flexure. Thus, it was ensured that after the flexural strengthening, the flexural capacity of the beam remains less than the enhanced shear capacity. The flexural strengthening was carried out in beam by providing CFRP in a manner similar to that of BWF. For CWS the specimens under this category were strengthened similar to the earlier specimens. In order to strengthen the shear deficient control specimens, the strengthening in the column was done with GFRP. This strengthening scheme enhanced the shear capacity of the column. To maintain a similar trend to that of the other type of specimens, nominal flexural strengthening in the column was also carried out by CFRP. The joint was also adequately strengthened with one layer of GFRP. The typical strengthening process is shown in Fig. 6b.

3. Results and discussion

3.1 Failure pattern

The failure modes and the extent of damage inflicted on the test specimens due to cyclic loading are presented in Fig. 7. In the early stage of cyclic loading, the first cracks in all the specimens mainly developed at the beam-column joint interface. With further increase in loading, the cracks propagated towards their weakest shear zone or the flexural zone or widening up the initial cracks at the joint face.

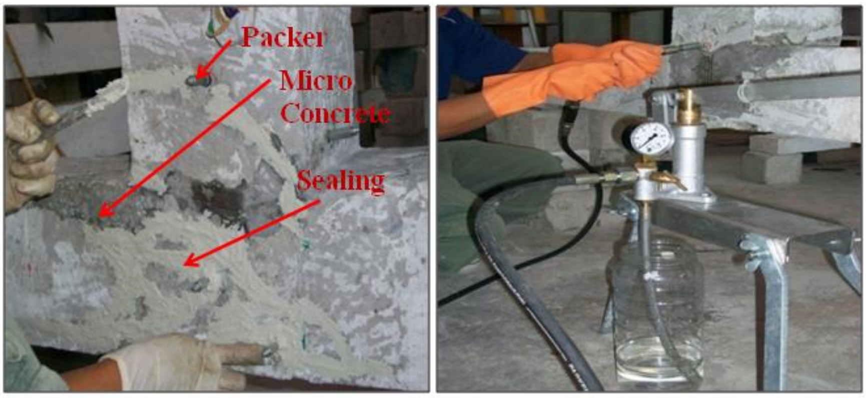

Fig. 5 Repairing of damaged beam-column connections

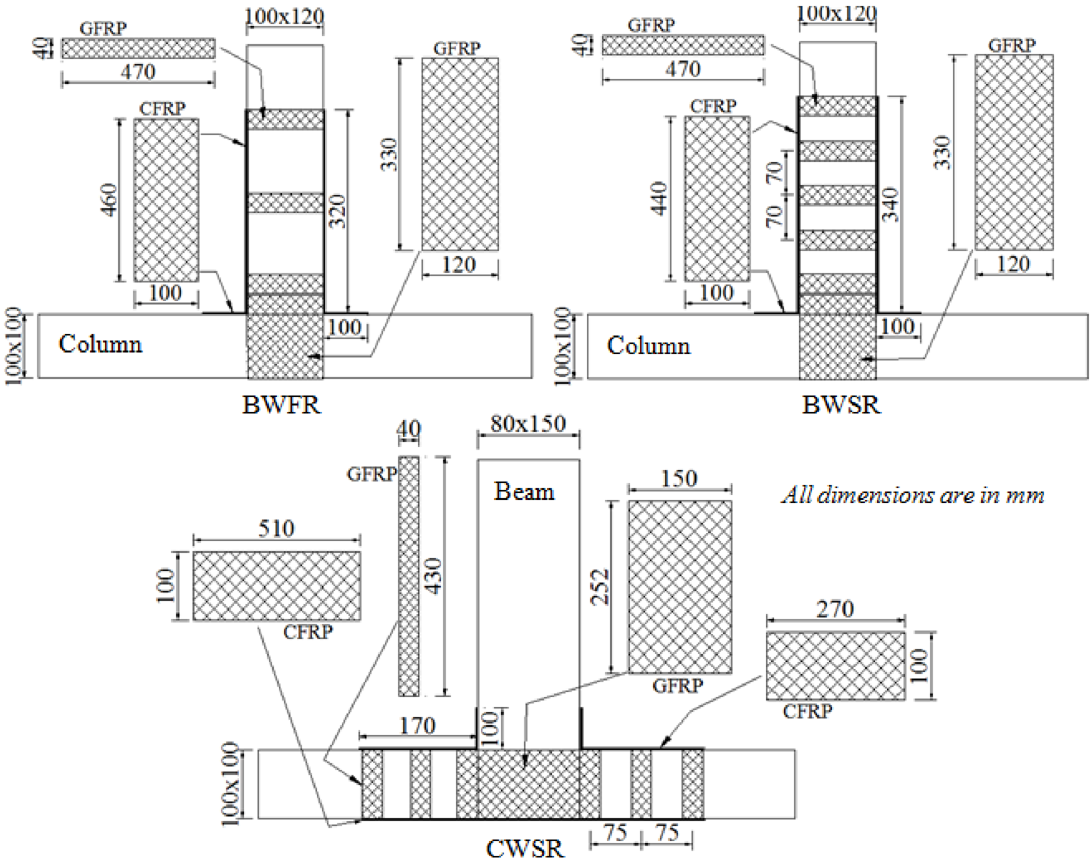

(a) Configuration of FRP sheet

(b) Wrapping of specimens using FRP sheet

Fig. 6 Strengthening of damaged beam-column connections

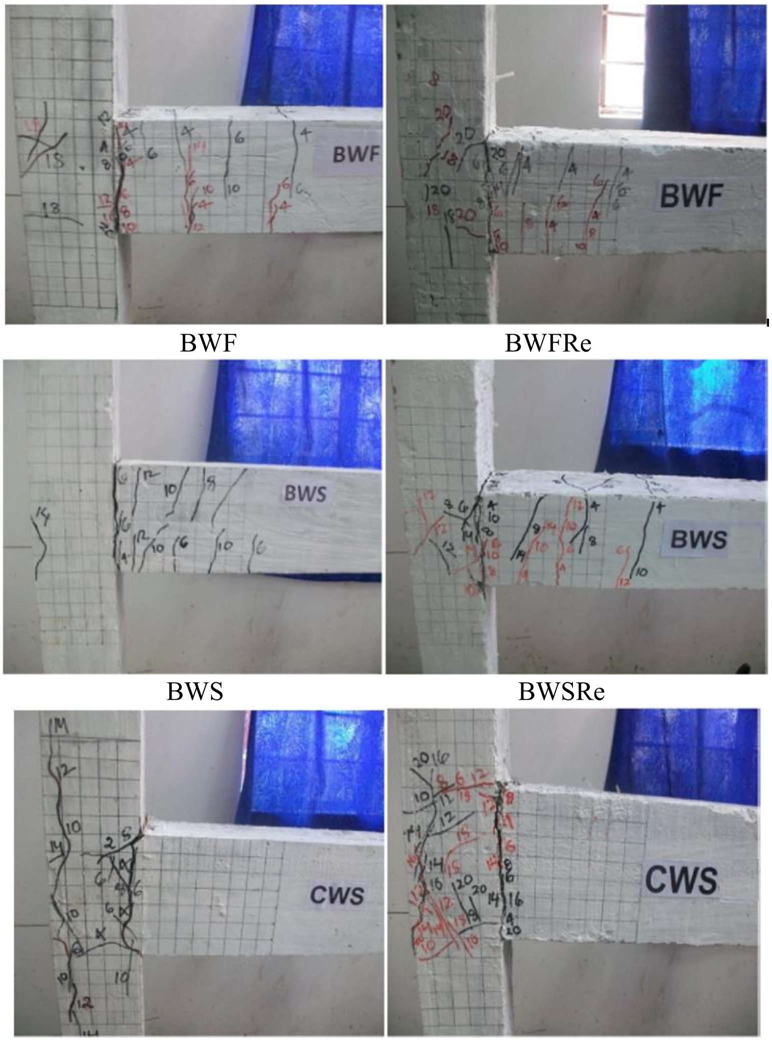

BWF BWFRe

BWS BWSRe

CWS CWSRe

Fig. 7 Damaged patterns of control and epoxy injected specimens

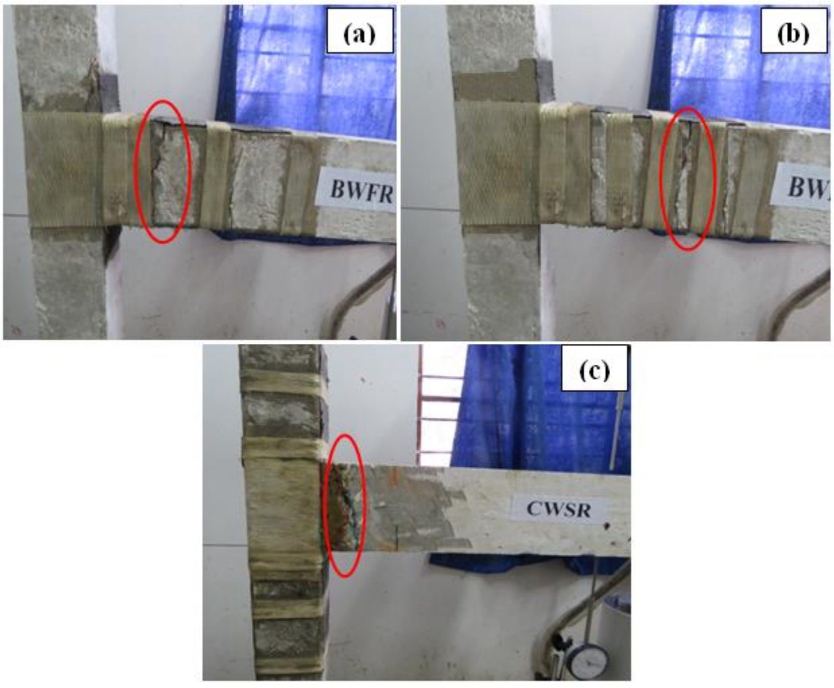

Fig. 8 Strengthened specimens (a) BWFR (b) BWSR and (c) CWSR

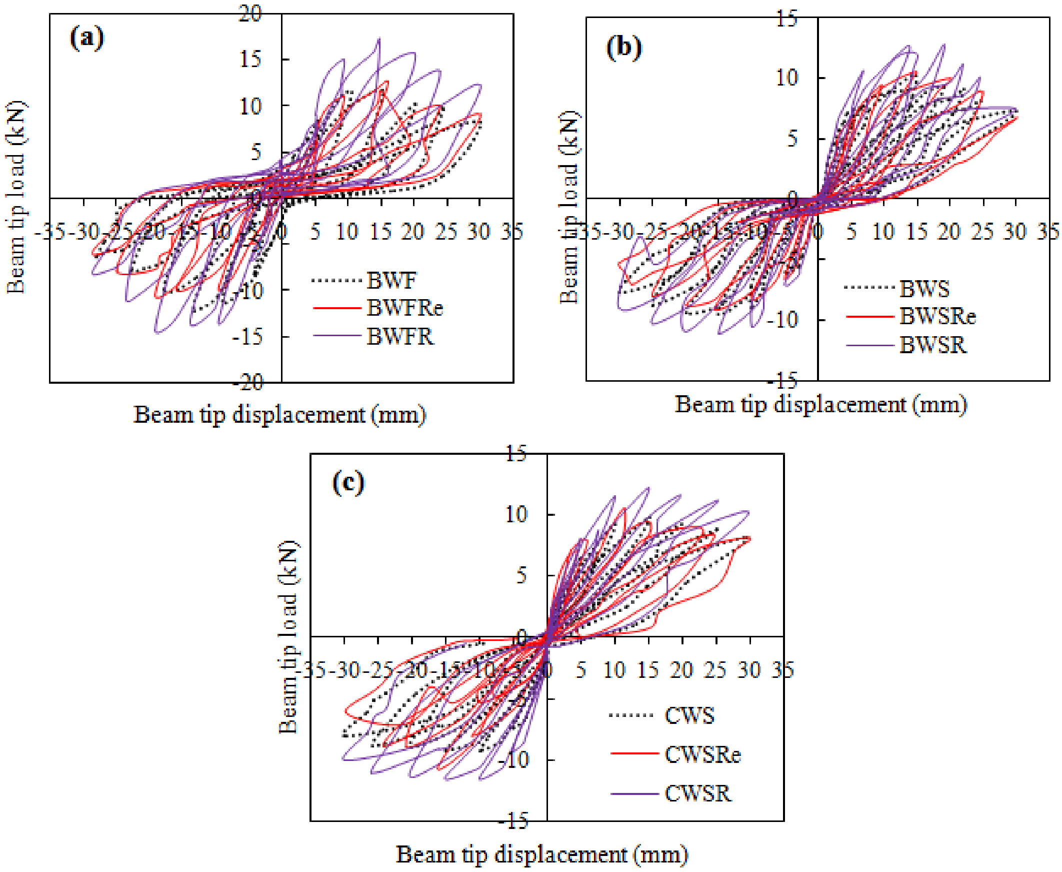

Fig. 9 Hysteresis loops (a) BWF (b) BWS and (c) CWS

A maximum crack width of about 5 mm was observed at the joint interface of the specimens. More number of cracks appeared in the rehabilitated specimens. Rehabilitated specimens undergo more displacement level and presented slightly higher ultimate loads carrying capacity as compared to the reference specimens. This shows that the adopted rehabilitation strategy was effective in retrieving the original load capacity. However, it may be observed from the Fig. 7 that more number of cracks appeared in rehabilitated specimens, which indicates that epoxy injection and micro concrete repairing is not able to improve the damaged pattern. The wrapping of FRP sheets designed as per configuration of the deficiency type however, not only enhanced the load carrying capacity but also improved the failure pattern. As observed in Fig. 8, flexural failure in beam occurs in both BWFR and BWSR however no damaged occur in column for CWSR and instead the crack shifted to the beam part. The formation of plastic hinged away from the joint region is a desirable failure mode for stability of an RC frame.

3.2 Hysteretic response of specimens

The typical hysteretic response obtained by plotting the test data is presented in Fig. 9. Various seismic parameters such as ultimate strength, energy dissipation, stiffness degradations and ductility of the specimens were evaluated from these hysteretic responses. Capacity comparison of specimens presented in Table 2 show marginally increase for epoxy injected specimens (10%, 2% and 8% for BWFRe, BWSRe and CWSRe respectively) and higher when confined with FRP sheets (48%, 20% and 40% for BWFR, BWSR and CWSR respectively) as compared to control specimens. The behaviors of these connections were studied by comparing these parameters. Rehabilitated and strengthened beam-column connections exhibited similar responses as compared to the reference specimens. The envelope curves as obtained from hysteresis loops are shown in Fig. 10. Comparing these curves of (control and rehabilitated of corresponding specimens type) at each displacement, it can be observed that all the rehabilitated specimens show a similar load displacement characterization with the initial slope being relatively lower. The envelope of hysteresis loops of the rehabilitated specimens, however, show slightly higher load-carrying capacity in both push and pull directions. Thus, all damaged control specimens could successfully restore the load-carrying capacity after rehabilitation. The wrapping of FRP sheets further enhanced the load-carrying at each displacement level. This study shows that the appropriately chosen repair strategy could retrieve back the lost capacity of damaged structural component for post earthquake usage. Higher load carrying capacity can be further achieved by appropriate strengthening. Thus, it may be inferred that the applied repair techniques are effective in restoring the load-carrying capacity of the vital beam-column connections.

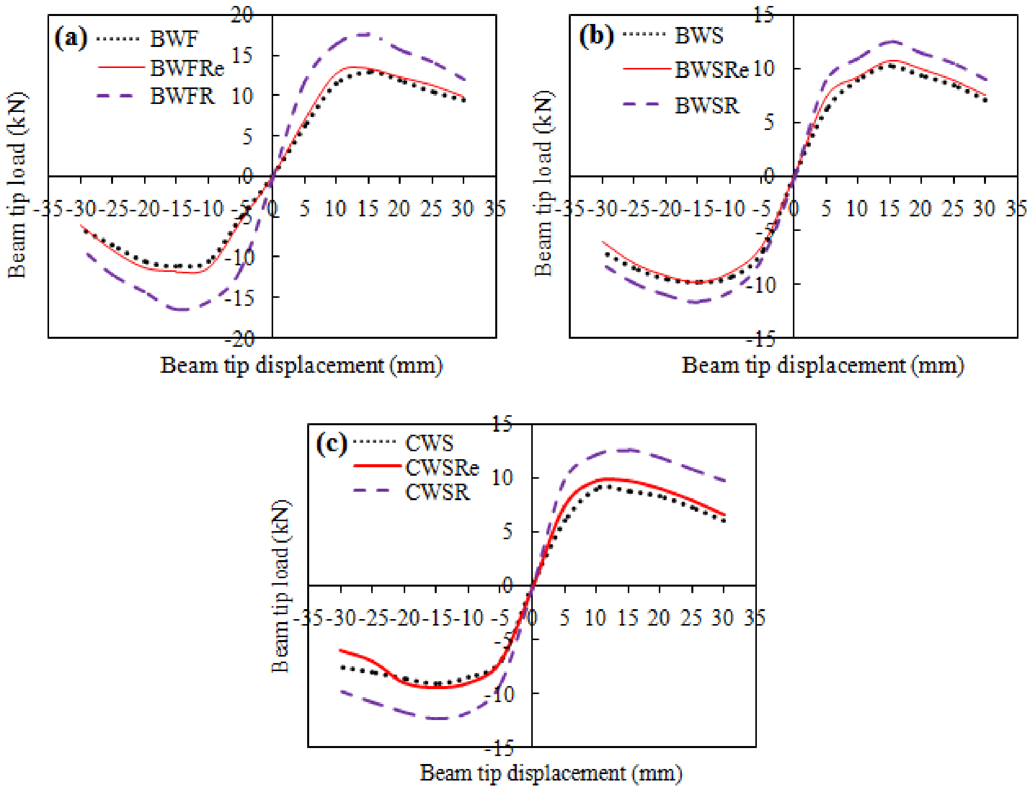

Fig. 10 Envelope of hysteretic loops (a) BWF (b) BWS and (c) CWS

3.3 Stiffness degradation

Secant stiffness is evaluated as the peak-to-peak stiffness of the beam tip load-displacement relationship. The secant stiffness is an index of the response of the specimen during a cycle and its strength degradation from a cycle to the following cycle. It is calculated as the slope of the line joining the peak of positive and negative capacity at a given cycle. The slope of this straight line is the stiffness of the assemblage corresponding to that particular amplitude (Naeim and Kelly 1999). The typical stiffness degradation of the test specimens is presented in Fig. 11. Irrespective of the deficiency types, they showed a similar degradation trend. Rehabilitated specimens of all types presented a slightly lower degradation trends. While, strengthen specimens presented a higher stiffness as compared to rehabilitated specimens. This improved the stiffness degradation of the specimens.

3.4 Cumulative energy dissipation

The performance of a structural element during seismic excitation depends to a large extent on its capacity to dissipate energy. The area of hysteresis loop is a measure of the energy dissipated. The cumulative energy dissipated at particular amplitude was calculated by summing up the energy dissipated in all the preceding cycles including that amplitude. The energy dissipation of specimens is presented in Table 2 and their variation with drift angle is presented in Fig.12. Due to the confinement of FRP strengthen specimens showed higher energy dissipation capacity as compared to rehabilitated specimens. As compared to the control specimens the increase in energy dissipation is about 41%, 27% and 48% for BWFR, BWSR and CWSR respectively. However, rehabilitated specimens are marginal higher about 9%, 5% and 7% for BWFRe, BWSRe and CWSRe than the control specimens. The increase in stiffness at the end of imposed displacement history attracted more load corresponding to any drift angle due to high strength epoxy resin injected into the damaged zone and FRP confinement, which prevent the initial crack propagations. Thus, the total area enclosed by the plot of beam tip load versus beam tip displacement was more. This was perhaps the reason for improvement in cumulative energy dissipation in the subsequent loading cycles.

3.5 Displacement ductility

The displacement ductility, which is the ratio between the ultimate displacements (d_u) to the displacement at first yield (d_y) was calculated for all the specimens following the method used by Shannag *et al.* (2005) which has been explained in Fig. 13. The ultimate displacement (d_u) was set at a displacement corresponding to 20% drop of peak load for computation. The yield displacement is calculated as the point of intersection between two straight lines drawn in the envelope curve. The first line is obtained by extending the line joining the origin and 50 % of ultimate load capacity point on positive and negative sides of the envelope curve, while the second line is obtained by drawing a horizontal line through the 80 % of ultimate load capacity point on either side. In the Fig. 13, dy_1 and dy_2 represent the yield

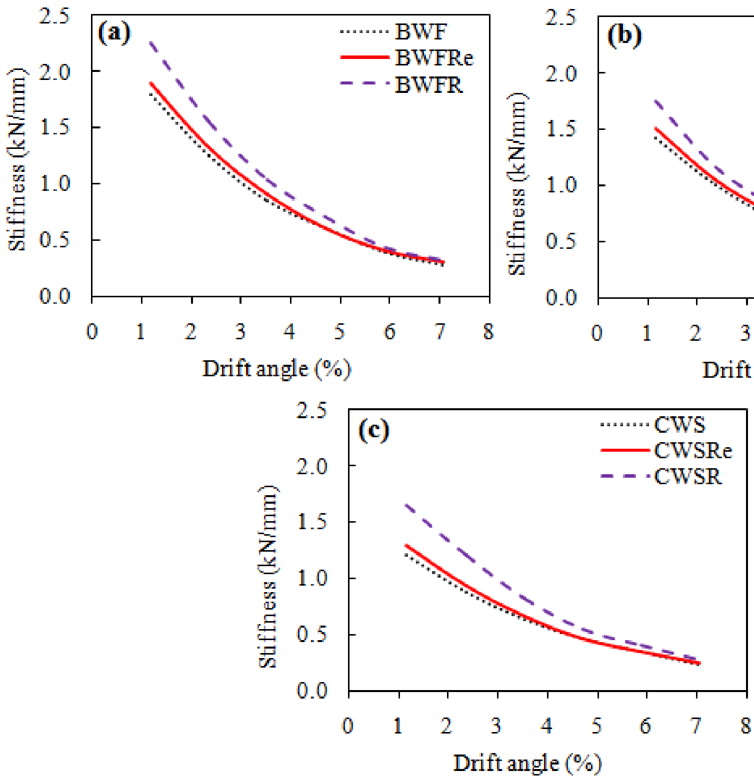

Fig. 11 Stiffness degradation (a) BWF (b) BWS and (c) CWS specimens

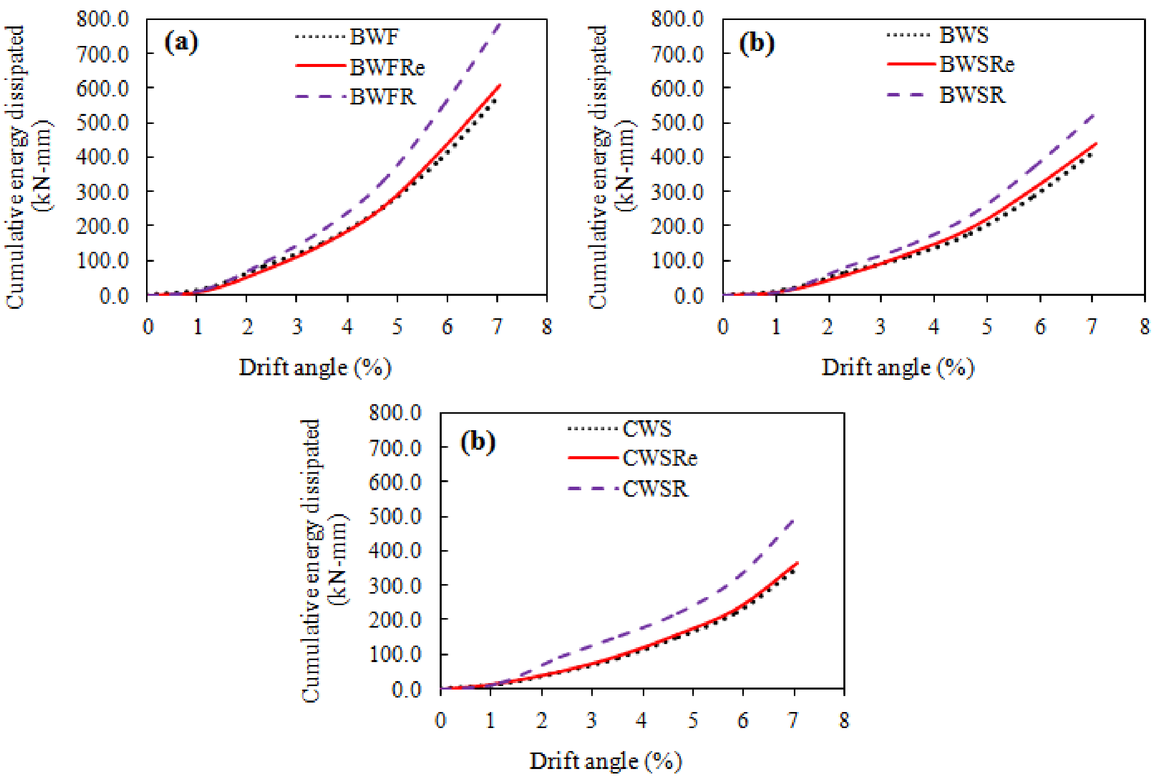

Fig. 12 Cumulative energy dissipation of beam-column specimens

displacement in positive and negative direction on the envelope curve respectively. The average value of yield displacement as obtained from both positive and negative direction is calculated. Horizontal lines drawn through the 80% of ultimate load capacity point on positive and negative side intersect the envelope curve at far end at points x_1 and x_2. The average of abscissa of these two points (denoted by du_1 and du_2 in Fig. 13) is taken as maximum displacement. The displacement ductility is calculated as the ratio of maximum displacement to the yield displacement and values are presented in Table 2. Irrespective of the deficiency types the displacement ductility attained by strengthen specimens are highest as compared to the rehabilitated specimens. Nevertheless, rehabilitated specimens are marginal higher than the control specimens which confirm the effectiveness of the repairing strategy.

3.6 Nominal principal tensile stresses

To have a better understanding of their behavior, nominal principal tensile stresses in beam-column joint region (damaged regions) were evaluated and compared in Fig. 14. From this figure it is can be deduced that the developed nominal principal tensile stresses of all control specimens are slightly lower than those of the rehabilitated specimens. However, the ability of high strength epoxy resin to prevent the crack propagation during cyclic loading; all rehabilitated specimens marginally increased the nominal principal tensile stresses of the specimens. This shows the effectiveness of epoxy repair to restore the tensile stress of the damaged connections to the original state. The confinement provided by FRP further increased the nominal principal tensile stresses of all strengthened specimens.

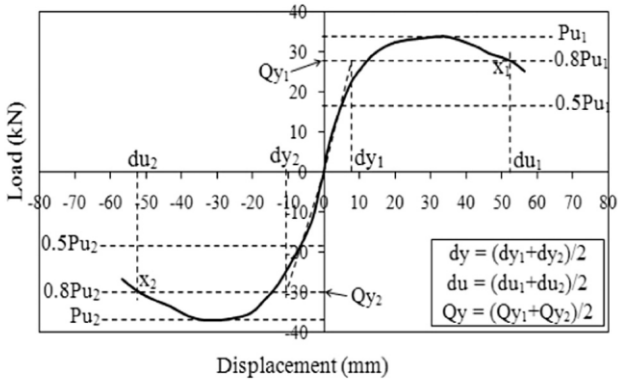

Fig. 13. Procedures for ductility calculation

4. Assessment of damaged control and rehabilitated specimens

4.1 Seismic damage index

Damage indices are intended to be used as numerical indicators of damage of any structural element under any loading type. Parameters such as strain, displacement, strength, energy and intrinsic dynamic properties are used to calculate these damage indices. The choice of an appropriate damage index may vary with the application. Williams and Sexsmith (1995) described Park and Ang

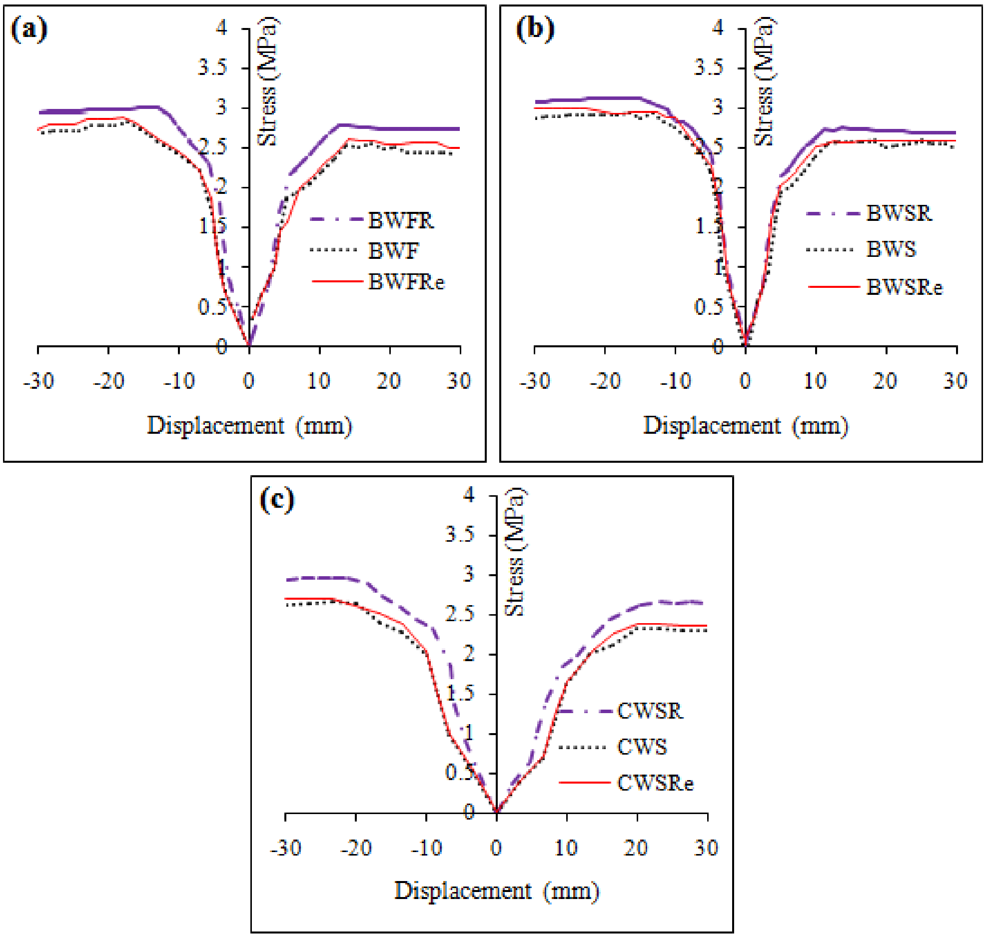

Fig. 14 Nominal principal tensile stress developed in beam-column joint region (a) BWF (b) BWS and (c) CWS specimens

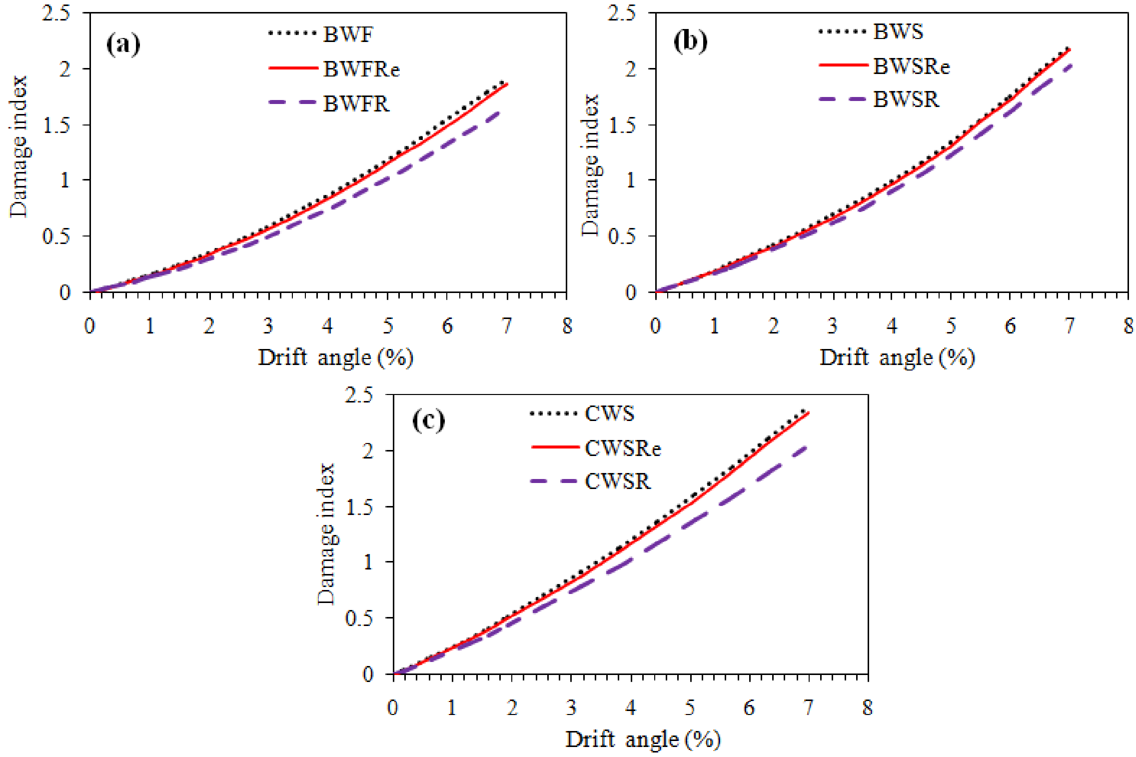

Fig. 15 Comparison of damage indices (a) BWF (b) BWS and (c) CWS

(1985) damage index as the most accurate representation of damage development among all the available cumulative damage index models. This damage index model has been widely used in recent years because of its simplicity and more so due to the fact that it has been calibrated using experimental data from various structures damaged during the past earthquakes. Damage index model of Park and Ang (1985) given in Eq. 1 was employ in this study to evaluate the damage level of the specimens.

$$DI = \frac{\delta_m}{\delta_u} + \frac{\beta}{\delta_u Q_y} \int dE \qquad (1)$$

where δ_m the maximum deflection attained during seismic loading, δ_u is the ultimate deflection capacity under monotonic load, Q_y is the yield force, dE is the incremental dissipated hysteretic energy and β is the strength degradation parameters. Parameters involved in the evaluation of the damage index were estimated as per Karayannis *et al*. (2008). The calculated damage indices for all specimens based on the above model are presented in Fig. 15. These figures show that the damage indices increase as the damage of specimens grow further with increased drift values. Further, all the curves of the damage indices are nearly linear, which suggest that the growth of damages in different specimens were stable. The lower damage index presented by rehabilitated and strengthened specimens indicated an effectiveness of the adopted rehabilitation and strengthening strategy.

4.2 Ultrasonic pulse velocity testing

Ultrasonic scanning is a recognized non destructive test method to assess the homogeneity and integrity of concrete structure. Assessment of control and rehabilitated specimens before and after rehabilitation using Ultrasonic Pulse Velocity (UPV) test were carried out and UPV values were used as indicators of damage status. It was observed that in most of the locations, the UPV values from the control specimen after damage were below 3.0 km/s. The UPV values below 3.0 km/s indicate that the qualities of the concrete at these zones are doubtful as per guidelines given by IS: 13311 (1992). However, after rehabilitations it has been observed that the UPV values improved considerably in the same location. Thus, it may be inferred that the cracks could be filled up by the injected epoxy. The UPV values after rehabilitation were above 3.2 km/s. Thus, it indicated that the quality of concrete fall in the good to excellent scale as per quality assessment guidelines. UPV tests were also done on the undamaged zone of each specimen for comparison purpose. Thus, this knowledge about the UPV values on the undamaged and damaged zones of control as well as rehabilitated specimen provided a very important platform for comparative analysis regarding the effectiveness of rehabilitation and also to reliably assess the condition of damaged concrete before rehabilitation.

5. Conclusions

Comparative studies covering various common types of beam-column connection with beam weak in flexure, beam weak in shear, and column weak in shear were addressed in this article. Various parameters related to seismic capacity

Table 2 Capacity comparisons of RC beam-column connections

Specimens type	Average load capacity, kN (+ve and –ve)	Increase with respect to control specimen (%)	Energy dissipation (kN-mm)	Increase with respect to control specimen (%)	Ductility (d_u-d_y)	Increase with respect to control specimen (%)
BWF	11.51	-	560	-	3.23	-
BWFRe	12.68	10	610	9	3.56	10
BWFR	17.05	48	790	41	5.87	82
BWS	10.05	-	418	-	2.84	-
BWSRe	10.28	2	440	5	3.11	10
BWSR	12.06	20	532	27	3.44	21
CWS	8.91	-	340	-	2.75	-
CWSRe	9.63	8	364	7	2.86	4
CWSR	12.44	40	502	48	4.25	55

were evaluated and performances of these rehabilitated specimens were evaluated by comparing its results with those obtained from the respective control specimens. Based on experimental studies carried out, the following conclusions have been drawn.

- An epoxy repair specimens is not able to improve the failure mode of the specimens. The combination of epoxy resin injection and FRP sheet wrapping change the mode of failures for BWS and CWS specimens significantly.
- Comparison of important parameters related to seismic capacity such as ultimate load, stiffness degradation, energy dissipation, and ductility showed that the adopted rehabilitation strategies were satisfactory as damaged beam-column connections after rehabilitation exhibited equal or marginally better performance. Further, seismic parameters improved by a combination of epoxy resin injection and FRP sheet wrapping.
- Rehabilitated specimens presented lower damage indices as compared to that of the corresponding control specimen. In addition, damage indices further reduce in all strengthened specimens.
- Nominal principal tensile stresses of all strengthened specimens are substantially increased in comparison with those of the corresponding rehabilitated specimens. Nevertheless, rehabilitated specimens are marginal higher than the control specimens.

Acknowledgments

Author acknowledges the financial assistance provided by Department of Science and Technology (DST), Government of India under the research grant DST NO. SB/EMEQ-498/2014 Dated: 26-06-2014.

References

ACI 352R-02 (2002), *Recommendations for Design of Beam-Column Connections in Monolithic Reinforced Concrete Structures*, American Concrete Institute, Farmington Hills, MI, USA.

ACI Committee 440.2R (2002), "Guide for the Design and Construction of Externally Bonded FRP Systems for Strengthening Concrete Structures", *American Concrete Institute*, Farmington Hills, MI, USA.

Alsayed, S.H., Al-Salloum, Y.A., Almusallam, T.H., and Siddiqui, N. A. (2010), "Seismic response of FRP-upgraded exterior RC beam-column joints", *J. Compos. Construct. ASCE*, **14**(2), 195-208. https://doi.org/10.1061/(ASCE)CC.1943-5614.0000067.

Ascione, F. Lamberti, M. Razaqpur, A.G and Spadea, S. (2017), "Strength and stiffness of adhesively bonded GFRP beam-column moment resisting connections", *Compos. Struct.*, **60**, 1248–1257. https://doi.org/10.1016/j.compstruct.2016.11.021.

Barbhuiya, S. and Choudhury, A.M. (2015), "A study on the size effect of RC beam-column connections under cyclic loading", *Eng. Struct.*, **95**, 1-7. https://doi.org/10.1016/j.engstruct.2015.03.052.

Choudhury, A.M., Deb, S.K. and Dutta, A. (2013), "Study on size effect of fibre reinforced polymer retrofitted reinforced concrete beam–column connections under cyclic loading", *Canadian J. Civil Eng.*, **40**(4), 353-360. https://doi.org/10.1139/cjce-2012-0041.

Corazao, M. and Durrani, A. J. (1989), "Repair and strengthening of beam-to-column connections subjected to earthquake loading", *NCEER-89-0013*, National Center for Earthquake Engineering Research, State University of New York at Buffalo, NY, USA.

Engindeniz, M. Kahn, L. F. and Zureick, A. (2005), "Repair and strengthening of reinforced concrete beam- column joints: State of the art" *ACI Struct. J.*,**102**(2), 187–197. https://doi.org/10.1061/(ASCE)CC.1943-5614.0000290.

Eslami, A. and Ronagh, H.R. (2014), "Experimental investigation of an appropriate anchorage system for flange-bonded carbon fiber–reinforced polymers in retrofitted RC beam–column joints", *J. Compos. Construct.,* **18**(4), 1-11. https://doi.org/10.1061/(ASCE)CC.1943-5614.0000456.

Federal Emergency Management Agency (FEMA) (1998), *Repair of Earthquake Damaged Concrete and Masonry Wall Buildings*, FEMA, USA. 24-42.

Ghobarah, A. and Said, A. (2002), "Shear strengthening of beam-column joints", *Eng. Struct.*, **24**(7), 881-888. https://doi.org/10.1016/S0141-0296(02)00026-3.

Ghobarah, A. Aziz, A. and Biddah, T. S. (1997), "Rehabilitation of reinforced concrete frame connections using corrugated steel jacketing", *ACI Struct. J.*, **4**(3), 283-294.

Hadi, M.N.S. and Tran, T.M. (2016), "Seismic rehabilitation of reinforced concrete beam–column joints by bonding with concrete covers and wrapping with FRP composite", *Mater.*

Struct., **49**(1–2), 467-485. https://doi.org/10.1617/s11527-014-0511-4.

IS 10262 (2009), *Guidelines for Concrete Mix Design Proportioning (CED 2: Cement and Concrete)*, Bureau of Indian Standard New Delhi, India.

IS 12269 (1087), *Specification for OPC-53 Grade Cement*, Bureau of Indian Standard, New Delhi, India.

IS 13920 (2016), *Ductile Detailing of Reinforced Concrete Structures Subjected to Seismic Forces - Code of Practice*, Bureau of Indian Standard New Delhi, India.

IS 1608 (1995), *Mechanical Testing of Metals - Tensile Testing*, Bureau of Indian Standard New Delhi, India.

IS 2386a (1993), *Methods of Test for Aggregates for Concrete - Part 1: Particle Size and Shape*, Bureau of Indian Standard, New Delhi, India.

IS 2386b (1963), *Methods of Test for Aggregates for Concrete - Part 3: Specific gravity, Density, Voids, Absorption and Bulking*, Bureau of Indian Standard, New Delhi, India.

IS 432 (1) (1982), *Specification for Mild Steel and Medium Tensile Steel Bars and Hard-Drawn Steel Wire for Concrete Reinforcement: Part I Mild Steel and Medium Tensile Steel Bars*, Bureau of Indian Standard New Delhi, India.

IS 456 (2000), *Plain and Reinforced Concrete - Code of Practice*, Bureau of Indian Standard New Delhi, India.

Kakaletsis, D.J., David, K.N. and Karayannis, C.G. (2011), "Effectiveness of some conventional seismic retrofitting techniques for bare and infilled R/C frame", *J. Struct. Eng. Mech.*, **39**(4), 499-520. https://doi.org/10.12989/sem.2011.39.4.499.

Karayannis, (2015), "Mechanics of external RC beam-column joints with rectangular spiral shear reinforcement: experimental verification", *J. Mechanica*, **50**(3), 311–322. https://doi.org/10.1007/s11012-014-9953-6.

Karayannis, C.G, Chalioris, C. E, and Sirkelis, G. M. (2008), "Local retrofit of exterior RC beam-column joints using thin RC jackets-An experimental study", *Earthq. Eng. Struct. Dynam.*, **37**, 727-746. https://doi.org/10.1002/eqe.783.

Karayannis, C.G. and Sirkelis, G.M. (2008), "Strengthening and rehabilitation of RC beam-column joints using C-FRP jacketing and epoxy resin injection", *J. Earthq. Eng. Struct. Dynam.*, **37**, 769-790. https://doi.org/10.1002/eqe.785.

Karayannis, C.G. Chalioris, C.E. and Sideris, K.K. (1998), "Effectiveness of RC beam-column connection repair using epoxy resin injections", *J. Earthq. Eng.*, **2**(2), 217-240.

Karayannis, C.G., and Sirkelis, G.M. (2002), "Effectiveness of RC beam-column connection strengthening using Carbon-FRP Jackets", *12th European Conference on Earthquake Engineering*, London, September.

Marthong, C., Dutta, A. and Deb, S.K. (2013), "Seismic rehabilitation of RC exterior beam-column connections using epoxy resin injection", *J. Earthq. Eng.*, **17**(3), 378-398. https://doi.org/10.1080/13632469.2012.738284.

Marthong, C., Dutta, A. and Deb, S.K. (2016), "Effect of Cyclic Loading Frequency on the Behavior of External RC Beam-Column Connections", *J. Earthq. Eng.*, **20**, 1126–1147. https://doi.org/10.1080/13632469.2016.1138164.

Mosallam, A.S. (2000), "Strength and ductility of reinforced concrete moment frame connections strengthened with quasi-Isotropic laminates", *Compos. Part B Eng.*, **31**(6-7), 481-497. https://doi.org/10.1016/S1359-8368(99)00068-2.

Mukherjee, A. and Joshi, M. (2005), "FRPC reinforced concrete beam-column joints under cyclic excitation", *Compos. Struct.*, **70**, 185-199. https://doi.org/10.1016/j.compstruct.2004.08.022.

Naeim, F. and Kelly, J.M. (1999), *Design of Seismic Isolated Structures from Theory to Practice*", Wiley, New Jersey, USA.

Panda K.C., Bhattacharyya S.K. and Barai S.V. (2013), "Shear strengthening effect by bonded GFRP strips and transverse steel on RC T-beams", *Struct. Eng. Mech.*, **4**(1), 75-98. http://dx.doi.org/10.12989/sem.2013.47.1.075.

Park, Y.J. and Ang, A.H.S. (1985), "Mechanistic seismic damage model for reinforced concrete", *ASCE*, **111**(4), 722-739. https://doi.org/10.1061/(ASCE)0733-9445(1985)111:4(722).

Saleh, H.A., Al-Salloum, A.Y., Almusallam, T.H. and Nadeem, A.S. (2010), "Seismic response of FRP-upgraded exterior beam-column joints", *J. Compos. Construct.*, **14**(2), 195-208. https://doi.org/10.1061/(ASCE)CC.1943-5614.0000067.

Sasmal, S., Ramanjaneyulu, K., Balthasar, N. Srinivas, V., Kumar, K.S., Korkowski, C., Roehm, C., Lakshmanan, N. and Iyer, N.R. (2010), "Seismic retrofitting of non ductile beam-column sub-assemblage using FRP wrapping and steel plate jacketing", *J. Construct. Build. Mater.*, **25**(1), 175-182. https://doi.org/10.1016/j.conbuildmat.2010.06.041.

Shannag, M.J. and Alhassan, M.A. (2005), "Seismic upgrade of interior beam-column sub-assemblages with high performance fiber reinforced concrete jackets", *ACI Struct. J.*, **102**(1), 131-138.

Tsonos, A.G. (2008), "Effectiveness of CFRP-Jackets and RC-Jackets in Post-earthquake and Pre-earthquake Retrofitting of Beam-Column Sub-assemblages", *Eng. Struct.*, **30**, 777-793. https://doi.org/10.1016/j.engstruct.2007.05.008.

Tsonos, A.G. (2014), "An innovative solution for strengthening of old R/C structures and for improving the FRP strengthening method", *Struct. Monitor. Maintenance*, **1**(3), 323-338. http://dx.doi.org/10.12989/smm.2014.1.3.323.

Uma, S.R. and Jain, S.K. (2006), "Seismic design of beam-column joints in RC moment resisting frames – Review of codes", *Struct. Eng. Mech.*, **23**(5), 579-597. https://doi.org/10.12989/sem.2006.23.5.579.

Vidjeapriya, R. and Jaya, K.P. (2013), "Experimental study on two simple mechanical precast beam-column connections under reverse cyclic loading", *J. Performance Construct. Facilities*, **27**(4), 402-414. https://doi.org/10.1061/(ASCE)CF.1943-5509.0000324.

William, M.S. and Sexsmith, R.G. (1995), "Seismic damage indices for concrete structures: A state-of-the-art review", *Earthq. Spectra*, **11**(2), 319-349. https://doi.org/10.1193/1.1585817.

CC